RESEARCH PAPER

NVP-QBE170: an inhaled blocker of the epithelial sodium channel with a reduced potential to induce hyperkalaemia

K J Coote[1], D Paisley[1], S Czarnecki[1], M Tweed[1], H Watson[1], A Young[1], R Sugar[1], M Vyas[1], N J Smith[1], U Baettig[1], P J Groot-Kormelink[1], M Gosling[1], R Lock[1], B Ethell[1], G Williams[1], A Schumacher[2], J Harris[2], W M Abraham[3], J Sabater[3], C T Poll[4], T Faller[1], S P Collingwood[1] and H Danahay[1,5]

[1]*Novartis Institutes for BioMedical Research, Horsham, UK,* [2]*Genomics Institute of the Novartis Foundation, San Diego, CA, USA,* [3]*Department of Research, Mount Sinai Medical Center, Miami, FL, USA,* [4]*Retroscreen Virology Ltd, London, UK, and* [5]*School of Life Sciences, University of Sussex, Brighton, UK*

BACKGROUND AND PURPOSE

Inhaled amiloride, a blocker of the epithelial sodium channel (ENaC), enhances mucociliary clearance (MCC) in cystic fibrosis (CF) patients. However, the dose of amiloride is limited by the mechanism-based side effect of hyperkalaemia resulting from renal ENaC blockade. Inhaled ENaC blockers with a reduced potential to induce hyperkalaemia provide a therapeutic strategy to improve mucosal hydration and MCC in the lungs of CF patients. The present study describes the preclinical profile of a novel ENaC blocker, NVP-QBE170, designed for inhaled delivery, with a reduced potential to induce hyperkalaemia.

EXPERIMENTAL APPROACH

The *in vitro* potency and duration of action of NVP-QBE170 were compared with amiloride and a newer ENaC blocker, P552-02, in primary human bronchial epithelial cells (HBECs) by short-circuit current. *In vivo* efficacy and safety were assessed in guinea pig (tracheal potential difference/hyperkalaemia), rat (hyperkalaemia) and sheep (MCC).

KEY RESULTS

In vitro, NVP-QBE170 potently inhibited ENaC function in HBEC and showed a longer duration of action to comparator molecules. *In vivo*, intratracheal (i.t.) instillation of NVP-QBE170 attenuated ENaC activity in the guinea pig airways with greater potency and duration of action than that of amiloride without inducing hyperkalaemia in either guinea pig or rat. Dry powder inhalation of NVP-QBE170 by conscious sheep increased MCC and was better than inhaled hypertonic saline in terms of efficacy and duration of action.

CONCLUSIONS AND IMPLICATIONS

NVP-QBE170 highlights the potential for inhaled ENaC blockers to exhibit efficacy in the airways with a reduced risk of hyperkalaemia, relative to existing compounds.

Abbreviations

P552-02, N-(3,5-diamino-6-chloropyrazine-2-carbonyl)-N'-4-[4-(2,3-dihydroxypropoxy)phenyl] butyl-guanidine; CF, cystic fibrosis; EIPA, 5-(N-Ethyl-N-isopropyl) amiloride; ENaC, epithelial sodium channel; FRT, Fisher rat thyroid; HBEC, human bronchial epithelial cell; I_{SC}, short-circuit current; MCC, mucociliary clearance; NHE, sodium hydrogen exchanger; NVP-QBE170, 1,4-Di-{4-[N'-(3,5-Diamino-6-chloro-pyrazine-2-carbonyl)-guanidino]-piperidine-1-carbonyl}-benzene; PHA, pseudohypoaldosteronism; TPD, tracheal potential difference

Tables of Links

TARGETS
Ion channels[a]
ENaC, epithelial sodium channel
NHE1, sodium hydrogen exchanger1 (SLC9A1)
Enzymes[b]
Na^+K^+-ATPase

LIGANDS
Amiloride
EIPA, 5-(N-ethyl-N-isopropyl) amiloride
Forskolin
P552-02
Phenamil
UTP

These Tables list key protein targets and ligands in this article which are hyperlinked to corresponding entries in http://www.guidetopharmacology.org, the common portal for data from the IUPHAR/BPS Guide to PHARMACOLOGY (Pawson et al., 2014) and are permanently archived in the Concise Guide to PHARMACOLOGY 2013/14 ([a,b]Alexander et al., 2013a,b).

Introduction

The epithelial sodium channel (ENaC) is composed of three subunits (αβγ) (Canessa et al., 1993) that are expressed in the apical membrane of several fluid absorptive epithelia including cortical collecting duct, colon and airway (Kellenberger and Schild, 2002). ENaC has been recognized as a drug target for the treatment of cystic fibrosis (CF) for approximately 30 years (Boucher, 2007). In the lungs, ENaC is responsible for the reabsorption of sodium ions out of the airway and with its osmotically obliged water (Knowles et al., 1981; Matsui et al., 1998). Airway mucosal hydration is critical for the formation of a mucus gel that can be transported by mucociliary clearance (MCC) and cough clearance, critical components of innate host defence in the lung (Boucher, 2007). In CF, there is a deficit of hydration in the airway resulting from either impaired or absent functioning of the CF transmembrane conductance regulator that is responsible for the secretion of both chloride and bicarbonate ions (Boucher et al., 1988; Quinton, 1989; Riordan et al., 1989; Matsui et al., 1998). As a consequence of this, mucus adheres to epithelial surfaces and MCC fails. Some studies have also suggested that ENaC activity is enhanced in the airway epithelium of CF patients although the interpretations of the data are controversial (Knowles et al., 1981; Boucher et al., 1988; Chen et al., 2010; Itani et al., 2011). Irrespective of whether ENaC is hyperactive in the CF airway, a blocker would be predicted to improve hydration and mucus clearance (Hirsh, 2002).

In support of this hypothesis, loss of function mutations in ENaC subunits can lead to the salt wasting disorder pseudohypoaldosteronism type 1 (PHA) (Chang et al., 1996; Strautnieks et al., 1996). PHA patients present with systemic electrolyte disturbances as a result of the loss of ENaC function in the kidney, but also show an airway MCC rate that is three- to fourfold the rate of a normal healthy individual (Kerem et al., 1999). Conversely, a transgenic mouse that over-expresses the β-subunit of ENaC on a lung-specific promoter develops a lung phenotype that includes plugging of the airways with mucus that fails to clear (Mall et al., 2004). In addition, the administration of topical amiloride to the airways of the newborn ENaC transgenics prevents the development of the mucus obstruction and subsequent lung inflammation and damage (Zhou et al., 2008). Together, these data support the central role that ENaC plays in the airway epithelium in regulating hydration and thereby affecting a critical component of innate host defence. Furthermore, a safe and well-tolerated ENaC blocker would be predicted to enhance innate defence in the CF lung and be of clinical benefit.

The potassium sparing diuretic amiloride (Figure 1A), an ENaC blocker, was demonstrated to enhance MCC in CF patients following inhalation (Köhler et al., 1986; App et al., 1990), although reports of clinical benefit have been variable between studies (Knowles et al., 1990; Graham et al., 1993; Bowler et al., 1995; Pons et al., 2000). It has been proposed that amiloride lacks the required potency and duration of action in the airway (Hofmann et al., 1997; Noone et al., 1997; Hirsh, 2002), properties that cannot be compensated for by simply increasing the dose as it is rapidly cleared by the kidney where target engagement induces hyperkalaemia (Perazella, 2000). When ENaC is blocked in the renal cortical collecting duct, sodium ions are no longer absorbed and potassium accumulates in the body. Two new ENaC blockers, P552-02 (Parion Sciences, Figure 1B) and GS9411 (Parion Sciences/Gilead, structure not disclosed), both amiloride analogues, have been specifically designed for inhaled dosing and show increased in vitro potency over amiloride (Hirsh et al., 2008). However, development of both candidates
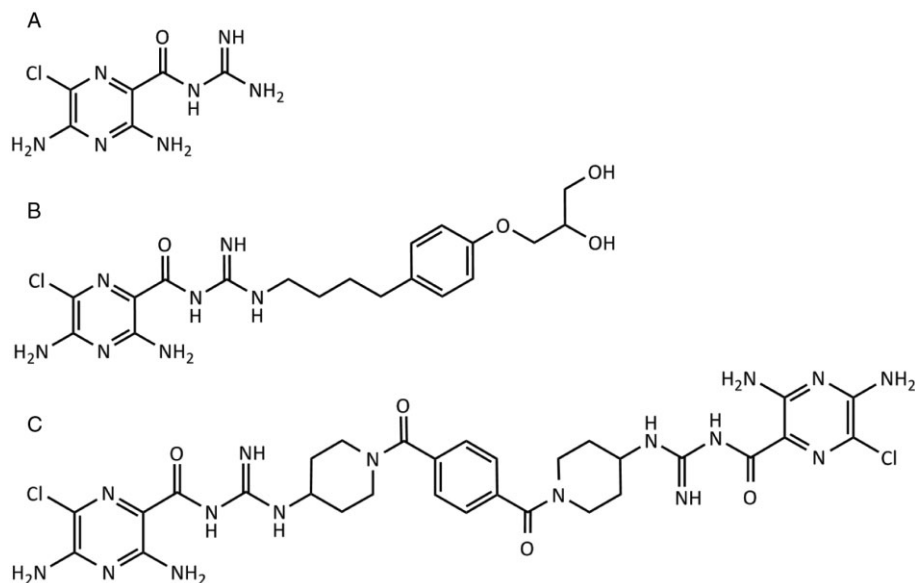
Figure 1
Chemical structures of amiloride (A) and the related ENaC blockers P552-02 (B) and NVP-QBE170 (C).

appears to have halted, with GS9411 having been reported to induce hyperkalaemia in clinical studies (O'Riordan *et al.*, 2014).

The goals of the present study were therefore to develop a novel class of ENaC blockers with substantially different properties to those previously described. Interesting compounds would retain potent activity *in vitro*, block airway ENaC and enhance MCC following inhalation *in vivo* and show evidence of a reduced potential to induce hyperkalaemia compared with amiloride and P552-02. To this end, we report on the preclinical properties of NVP-QBE170 (Figure 1C), a dimeric-amiloride derivative that shows a potent and selective block of ENaC both *in vitro* and *in vivo* with a significantly enhanced safety window over existing ENaC blockers, in terms of hyperkalaemia.

Methods

All animal care and experimental procedures were in accordance with the guidelines of the United Kingdom Home Office on the Operation of the Animals (Scientific Procedures) Act 1986 and were approved by the local Ethical Review Process or Swiss Animal Welfare law. Sheep studies were approved by the Mount Sinai Medical Center Animal Research Committee. The results of all studies involving animals are reported in accordance with the ARRIVE guidelines (Kilkenny *et al.*, 2010; McGrath *et al.*, 2010). A total of 228 animals were used in the experiments described here.

Male Dunkin Hartley guinea pigs (300–650 g) and male Sprague-Dawley rats (250–450 g) (Harlan, UK) were used during the course of these studies. Animals were acclimatized for a minimum of 7 days before study, maintained on a 12 h light-dark cycle at a temperature of 21 ± 2°C and humidity of

55 ± 5%. Animals were allowed food (guinea pigs: FD1 pellets, SDS, UK; rats: RM1P, Lillico, Aylesford, UK), hay (autoclavable hay bales, Lillico) and water *ad libitum*.

Cell culture

Human bronchial epithelial cell (HBEC) culture. HBECs (Lonza, Slough, UK) were cultured at an air-liquid interface (ALI) as previously described (Coote *et al.*, 2008). From the first day of establishment of an ALI, HBECs were fed with a DMEM : HAMS F-12 (1:1) media containing 2% Ultroser G (Pall BioSepra, Cergy, France) with gentamicin (50 µg·mL^{-1}) and amphotericin B (50 ng·mL^{-1}). Cells were used for short-circuit current (I_{SC}) assay between days 14 and 21 after the establishment of the ALI.

Transiently transfected human, rat and guinea pig ENaC in Fisher rat thyroid (FRT) cells. FRT cells were cultured in T162 cm^2 flasks with F-12 Ham nutrient mix supplemented with 10% FBS, 100 U·mL^{-1} penicillin and 100 µg·mL^{-1} streptomycin (growth media) at 37°C in a humidified atmosphere of 5% CO$_2$ (Sheppard *et al.*, 1994). FRT cells were transiently transfected with the plasmids encoding either rat or guinea pig ENaC subunits using Fugene 6 (Roche Biosciences, Burgess Hill, UK) as previously described (Coote *et al.*, 2008). For human ENaC subunits, either wild type or mutants encoding for modifications of key amiloride-binding sites (αβG525Aγ and αβγG537C) were transfected (Schild *et al.*, 1997). Transfections were performed in growth media further supplemented with amiloride (10 µM). After overnight transfection, the FRT cells were trypsinized and seeded onto filter inserts (1.65 × 10^5 cells per insert) using growth media supplemented with dexamethasone (30 nM) and amiloride (10 µM). The inserts were fed on both the apical and the basolateral sides on day 1 post seeding. Cells were used for I_{SC} assays on day 2.

I_{SC} and patch clamp assays

I_{SC} assay. At the stated time in culture, the ion transport properties of HBEC or transfected FRT cells were examined using the I_{SC} technique. Cells on Snapwell inserts were mounted on Vertical Diffusion Chambers (Harvard Apparatus, Cambridge, UK) and were bathed with continuously gassed Ringer solution (5% CO_2 in O_2; pH 7.4) maintained at 37°C containing (in mM): 120 NaCl, 25 $NaHCO_3$, 3.3 KH_2PO_4, 0.8 K_2HPO_4, 1.2 $CaCl_2$, 1.2 $MgCl_2$ and 10 glucose. The solution osmolality was always between 280 and 300 mosmol·kg⁻¹ H_2O for all physiological salt solutions used. Cells were voltage clamped to 0 mV (model EVC4000; WPI, Hitchin, UK) and the I_{SC} was measured. Transepithelial resistance (R_T) was measured by applying a 1 or 2 mV pulse at 30 s intervals and calculating R_T by Ohm's law. Data were recorded using a PowerLab workstation (ADInstruments, Oxford, UK). Direct ENaC blocker compounds were added to the apical chamber from a 1000-fold stock solution (prepared in DMSO) to achieve a cumulative concentration response in terms of the inhibition of the basal I_{SC}. At the completion of the concentration response, a supra-maximal concentration of amiloride (10 μM human; 30 μM guinea pig or rat) was added. IC_{50} values were calculated assuming that the cumulative current inhibition achieved with the test compound and supra-maximal amiloride reflected the total ENaC-mediated I_{SC}.

Washout assay. HBECs were mounted in Ussing chambers and short circuited as described above. Amiloride (20 μM) was then added to the apical chamber to establish the magnitude of the ENaC-mediated I_{SC}. Following a 2 min incubation, the apical chamber was perfused with fresh Ringers solution (5 mL·min⁻¹) and the I_{SC} recovered to the pre-amiloride level. At this time, the perfusion was stopped and the test ENaC blocker was added to the apical chamber at approximately 100× IC_{50} value (amiloride: 20 μM, NVP-QBE170: 700 nM, P552-02: 250 nM). Compounds were incubated with the HBEC for either 2 or 10 min and then the apical perfusion was restarted (washout) and recovery of the I_{SC} was measured. Washout of test compounds was quantified as the % recovery of the ENaC-mediated I_{SC} at 300 s after initiation of the apical perfusion.

Patch clamp assay. The sheep ENaC α1, β1 and γ1 subunit cDNAs were subcloned in the pXOON expression vector (Jespersen et al., 2002) and were transfected using Fugene 6 (Roche Biosciences). The intra- and extracellular solutions used for whole-cell patch clamp studies were Na⁺ ion selective, employing a Cs⁺-based intracellular solution to remove potentially contaminating K⁺ currents, as described by Staruschenko et al. (2006). Test compounds were constantly perfused in the extracellular solution and an IC_{50} value for the inhibition of the ENaC current was established. Additional methods are provided in the Supporting Information.

Guinea pig tracheal potential difference (TPD)

The methods for intratracheal (i.t.) dosing of guinea pigs and measurement of TPD have been previously described (Coote et al., 2008). In brief, animals were placed under short-acting anaesthesia [halothane (Merial, Harlow, UK)/

N_2O] to enable the i.t. instillation of test compounds or vehicle (0.2 mL in 5% dextrose). At either 1 or 4 h after compound dosing, animals were placed under surgical anaesthesia. Guinea pigs were first treated with 1 mL·kg⁻¹ (i.p.) Hypnovel® (5 mg·mL⁻¹ midazolam; Roche, Welwyn, UK) as a pre-anaesthetic agent followed 10 min later by a 1 mL·kg⁻¹ (i.p.) injection of Narketan10® (100 mg·mL⁻¹ ketamine; Vetoquinol, Buckingham, UK) and Rompun® (25 mg·mL⁻¹ xylazine; Bayer, Newbury, UK) in Water for Injections (Baxter Healthcare, Newbury, UK) mixed at a ratio of 2:1:1 respectively. The trachea was then exposed and an agar bridge electrode was placed into the lumen with a reference electrode placed into the soft tissue adjacent to the trachea. Potential difference measurements were taken via an IsoMil (WPI) through a PowerLab 16/S, and recorded on data capture software Chart for Windows (PowerLab, ADInstruments). At the completion of TPD measurements, a terminal blood sample was taken from the vena cava and blood potassium levels were measured using an IRMA TruPoint (LDH, UK; Abaxis, Dunnington, UK) with H3 cuvettes (LDH). Data are expressed as mean absolute potential difference or blood potassium values ± SEM.

Rat hyperkalaemia

Male Sprague-Dawley rats (250–350 g) were placed under short-acting anaesthesia and treated with test compounds by i.t. administration as described for guinea pigs (above). Blood samples were collected from the tail vein prior to compound administration and then at 6, 24 and 48 h after dosing. Blood potassium levels were measured immediately after sampling using the IRMA TruPoint system described above. To account for putative differences in the time course of blood potassium changes, the maximum level reached for each animal after compound administration was determined and compared with the equivalent maximum level for the vehicle-treated control group. In parallel studies, the pharmacokinetic profiles of NVP-QBE170 and P552-02 were studied. Briefly, rats were surgically implanted with a jugular vein cannula 48 h before drug administration. Test compounds (1 mg·kg⁻¹) were given i.v. and animals were placed in metabolism cages to collect urine. At defined time points up to 24 h after dosing, serial blood samples (300 μL) were collected into EDTA blood tubes via the implanted cannula. Following each blood sample, an equal volume of heparinized saline (10 IU·mL⁻¹ in normal saline) was infused back into the animal via the jugular vein cannula. Blood samples were centrifuged to separate plasma and 100 μL aliquots transferred to microtitre plates and then stored at –20°C until analysis by LC-MS/MS. For some studies, ¹⁴C labelled NVP-QBE170 was utilized.

Sheep MCC

MCC was measured in conscious sheep as previously described (Hirsh et al., 2008; Coote et al., 2009). Briefly, adult ewes (25–45 kg, Florida Native; 1–4 years old; Fair Meadows Farm, Ocala, FL, USA) were restrained in an upright position and were nasally intubated. Test compounds were delivered as dry powder lactose blends (Respitose SV003; DMV-Fonterra, Goch, Germany) using a Spinhaler device (Rhone-Poulenc Rorer Ltd., Dublin, Ireland). Hypertonic saline (7%)

and water control were administered to the sheep via the endotracheal tube by nebulization (3 mL). All aerosols were generated using a Raindrop Nebulizer (Nellcor Puritan Bennett, Carlsbad, CA, USA) which produces a droplet with a mass median aerodynamic diameter of approximately 1.1 μm. Aerosolized technetium labelled sulphur colloid (^{99m}Tc-SC; 20 mCi) was used to measure the effects of the various doses of test compounds or control on MCC by gamma scintigraphy. Animals were administered ^{99m}Tc-SC at the stated times following administration of test substances. Serial images were then obtained over a 2 h period at 5 min intervals for the first hour and then every 15 min for the next hours. Counts from the right lung were corrected for decay and expressed as a percentage of radioactivity cleared relative to the baseline image (% cleared). Differences in clearance of ^{99m}Tc-SC were compared at both 60 and 120 min after radio-aerosol administration. Additional methods are provided in the Supporting Information.

Data analyses

Unless stated otherwise, data sets were compared using a one-way ANOVA with a *post hoc* Dunnett's test for comparisons of compound effects to a single, common control group, with significance assumed when $P < 0.05$. Dose-response data were fitted using GraphPad Prism (GraphPad Software Inc., La Jolla, San Diego, CA, USA) and the concentration (IC_{50}) or dose (ED_{50}) required to induce 50% of the compound effect was calculated. Mean ^{99m}Tc-SC retention data were compared using a one-way ANOVA. A significant difference between groups was followed up with a Student–Newman–Keuls test to determine pairwise differences with significance assumed when $P < 0.05$.

Results

In vitro *activity*

NVP-QBE170 attenuated the amiloride-sensitive I_{SC} in HBEC with an IC_{50} of 6.9 nM ($n = 12$) (Supporting Information Fig. S1). Activity was also confirmed on guinea pig (30 nM) and rat (29 nM) ENaC following transient transfection into FRT cells and I_{SC} assay (Table 1). Sheep ENaC was transiently expressed in CHO cells and the IC_{50} for NVP-QBE170 was established using conventional patch clamp. Amiloride and P552-02 likewise attenuated ENaC function across species with potency values, comparable to published data (Coote *et al.*, 2008; Hirsh *et al.*, 2008).

Mutations of the human ENaC channel at sites reported to be important determinants of amiloride binding also shifted the potency of NVP-QBE170 (Table 2). αβG525Aγ and αβγG537C mutants shifted the amiloride IC_{50} by >1200- and 442-fold respectively (relative to wild-type channels). The NVP-QBE170 IC_{50} value was similarly shifted by >100-fold by both of these mutants, consistent with these residues playing a key role in the binding of the dimeric-amiloride derivative.

To determine the duration of action *in vitro*, HBECs in Ussing chambers were incubated with the ENaC blockers for

Table 1

In vitro potency of ENaC blockers

	pIC50			
Compound	**Human**	**Guinea pig**	**Rat**	**Sheep**
Amiloride	6.64 ± 0.14 (59)	6.53 ± 0.13 (27)	6.40 ± 0.15 (41)	6.73 ± 0.17 (3)
NVP-QBE170	8.27 ± 0.32 (12)	7.60 ± 0.27 (5)	7.57 ± 0.20 (4)	8.55 ± 0.31 (3)
P552-02	8.62 ± 0.15 (12)*	8.42 ± 0.31 (32)*	8.46 ± 0.18 (14)*	8.45 ± 0.42 (4)

Mean pIC_{50} data ± SD (n) for selected ENaC blockers on human ENaC (bronchial epithelial cells), guinea pig, or rat ENaC (transiently transfected into FRT cells) and sheep ENaC (transiently transfected into CHO cells). Values were calculated from I_{SC} assays (human, guinea pig and rat) or from patch clamp studies (sheep). *Data previously reported in Coote *et al.* (2008).

Table 2

The effects of amiloride-binding site mutations in human ENaC subunits on the potency of NVP-QBE170

	Wild type (αβγ)	**αβG525Aγ**		**αβγG537C**	
Compound	**pIC50**	**pIC50**	**Fold shift**	**pIC50**	**Fold shift**
Amiloride	6.85 ± 0.15 (3)	3.74 ± 0.04 (4)	1243	4.21 ± 0.17 (5)	445
NVP-QBE170	7.24 ± 0.15 (7)	5.26 ± 0.38 (5)	113	5.21 ± 0.26 (5)	116
P552-02	8.85 ± 0.19 (4)	5.21 ± 0.16 (6)	4316	6.19 ± 0.10 (7)	435

Mean pIC_{50} data ± SD (n) for selected ENaC blockers on both wild-type and mutated human ENaC (transiently transfected into FRT cells). Fold shifts are calculated using the mean IC_{50} for the defined mutant divided by the mean IC_{50} determined for the wild-type channel.

Figure 2

Duration of action of ENaC blockers on primary HBECs. ENaC-mediated I_{SC} was blocked with the test compounds and recovery of the current was measured during washout of compound from the apical side of the Ussing chamber. A sample raw data trace (A) illustrates the protocol whereby the magnitude of the ENaC-mediated I_{SC} was first established with amiloride (20 μM) that was then washed out of the chamber. The vertical arrow illustrates the 100% value for ENaC block. A supra-maximal concentration of the test compound (100× IC_{50}) was then added to the apical bath and incubated for either 2 or 10 min (a 2 min incubation is shown). The compound was then removed from the apical bath by constant perfusion and the duration of compound activity is measured as the recovery of the I_{SC}. Finally, amiloride was reintroduced to the apical bath to confirm that the recovered I_{SC} was ENaC mediated. Panels (B) and (C) illustrate mean % recovery data ± SEM (n = 6 independent experiments per compound) following either a 2 or 10 min incubation with test compound respectively.

either 2 or 10 min at a concentration 100× their IC_{50} and then an apical perfusion was activated to remove the compound (see Figure 2 for protocol). At 300 s following the start of perfusion, the blocking effect of amiloride on the I_{SC} had essentially disappeared, i.e., I_{SC} had recovered, after either a 2 or 10 min incubation (Figure 2; Table 3). In the case of NVP-QBE170, the block of ENaC was more persistent and I_{SC} recovery was related to the length of the incubation with the blocker (Table 3; $P < 0.05$ compared with time-matched amiloride controls). Compound P552-02 showed an intermediate duration of block, that was significantly different to both amiloride and NVP-QBE170 (Table 3; $P < 0.05$). See Supporting Information Fig. S2 for sample raw data traces.

In vivo *activity profile*

Guinea pig TPD. Intratracheal administration of NVP-QBE170 as a solution attenuated the TPD with an ED_{50} of 1.7 μg·kg^{-1}, when measured at 1 h after dosing (Table 4). We have previously reported ED_{50} values for amiloride (16 μg·kg^{-1}) and P552-02 (0.2 μg·kg^{-1}) in the identical model system 1 h after i.t. administration of the compounds as solutions (Coote *et al.*, 2008). We next extended these studies to examine the durability of the effects. In separate groups of animals, each of the three compounds was again given by i.t. administration but with the TPD assessment performed 4 h after dosing (Table 4 and Figure 3). Amiloride with doses of up to the maximum that could be formulated as a solution (5000 μg·kg^{-1}) failed to show any residual airway activity by 4 h after dosing. However, in the same animals, amiloride at doses ≥1670 μg·kg^{-1} did induce a significant elevation of blood potassium levels ($P < 0.05$; Figure 3D). NVP-QBE170 and P552-02 both showed residual airway effects at 4 h after dosing with ED_{50} values of 410 and 128 μg·kg^{-1} respectively (Figure 3B and C). In these same animals, P552-02 also significantly elevated blood potassium levels at doses ≥60 μg·kg^{-1} (Figure 3F). In contrast to both amiloride and P552-02, NVP-QBE170 did not change blood potassium levels up to and including the highest dose that could be formulated as a solution, 2000 μg·kg^{-1} (Figure 3E).

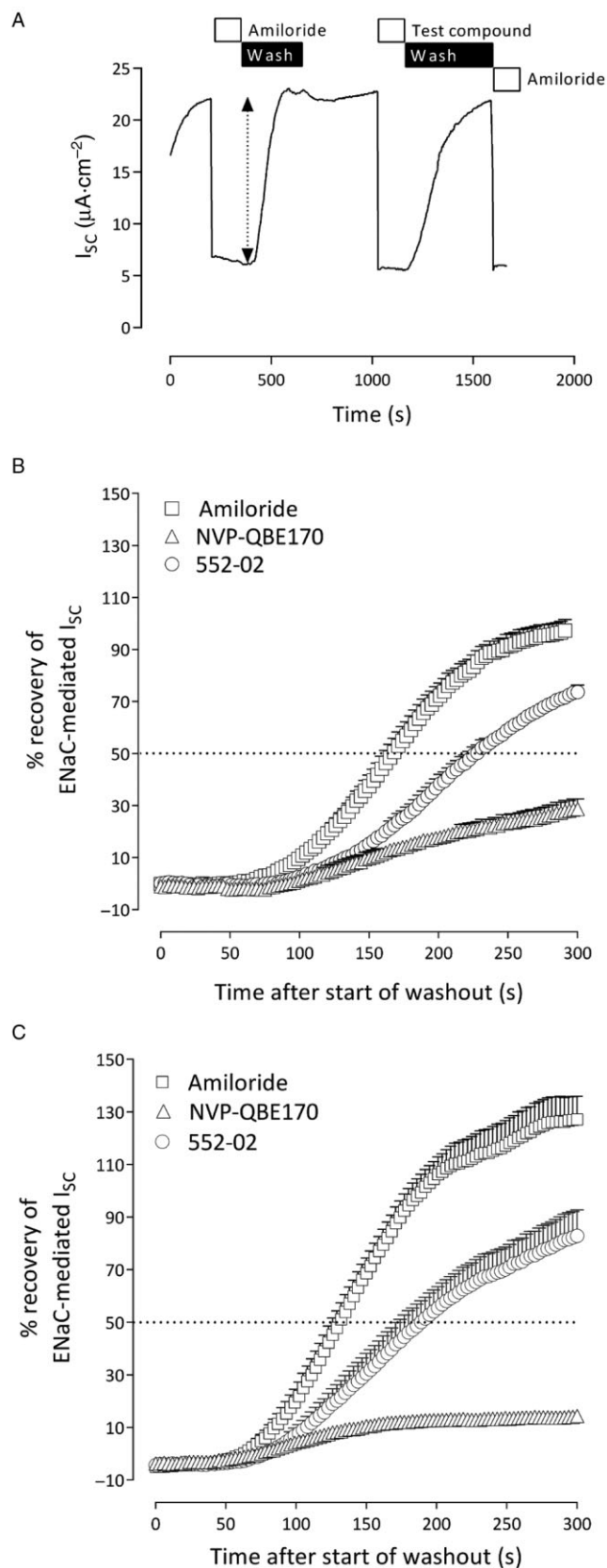*Rat model of hyperkalaemia.* Intratracheal dosing of ENaC blockers induced dose-dependent increases in blood potas-

Table 3

The effects of compound washout on the recovery of ENaC-mediated I_{SC} in cultured HBECs

Compound	Incubation time (min)	% recovery of I_{SC} at 300 s
Amiloride	2	97.3 ± 3.4
	10	127.1 ± 8.8
NVP-QBE170	2	28.7 ± 3.9*
	10	14.4 ± 1.8*
P552-02	2	73.7 ± 2.7*
	10	82.9 ± 9.9*

Mean % recovery data ± SEM are shown. The % recovery was calculated based upon the recovery of the test compound-mediated decrease in I_{SC} (see Figure 2A). *$P < 0.05$, significantly different from amiloride at the same incubation time; one-way ANOVA with *post hoc* Dunnett's test; $n = 6–9$ independent experiments per compound.

Table 4

The *in vivo* effects of ENaC blockers on guinea pig TPD and blood potassium levels following i.t. dosing

Compound	ED$_{50}$ (µg·kg^{-1}) 1 h	4 h	Max non-hyperkalaemic dose (µg·kg^{-1})[a]
Amiloride	16[b]	>5000	500
NVP-QBE170	1.7	410	≥2000
P552-02	0.2[b]	128	<60

The effects of ENaC blockers were evaluated for effects on the TPD in guinea pigs both at 1 and 4 h after i.t. instillation of a solution dose. Each study comprised group sizes of 4–10 animals within each treatment group. [a]Indicates the highest dose level that failed to induce a significant rise in blood K$^+$ levels above the vehicle control group. [b]Indicates data previously reported in Coote *et al.* (2008).

sium levels in rats that generally peaked at either 6 or 24 h after administration. To account for variability in the time of the peak increase, the maximum potassium level reached by each individual animal was used for quantification. Amiloride and P552-02 induced significant increases in blood potassium levels at doses of 2000 and 600 µg·kg^{-1} respectively (Table 5; Figure 4A and C). In contrast, NVP-QBE170 failed to induce an elevation of blood potassium levels at doses ≤3297 µg·kg^{-1} (Table 5; Figure 4B), the highest dose studied. When dosed by the i.t. route, once daily for 10 consecutive days, NVP-QBE170 again failed to induce a change in blood potassium levels (Figure 4D) at the highest dose studied (1000 µg·kg^{-1}·day^{-1}).

Sheep model of MCC. NVP-QBE170 was formulated as a dry powder blend in lactose (0–15% blends) and was administered to free-breathing adult ewes using a Spinhaler device.

Table 5

The effects of ENaC blockers on blood potassium levels in rats following i.t. dosing

Compound	Dose (µg·kg^{-1})	Maximum blood potassium level achieved following dosing (mmol·L^{-1})
Vehicle	–	5.75 ± 0.06
Amiloride	200	5.78 ± 0.09
	2000	6.09 ± 0.15*
	6000	6.82 ± 0.15*
NVP-QBE170	330	5.50 ± 0.12
	1099	5.66 ± 0.11
	3297	5.66 ± 0.08
P552-02	200	5.93 ± 0.20
	600	6.53 ± 0.08*
	2000	6.95 ± 0.18*

Blood potassium levels are expressed as the mean of the maximum level reached over the 48 h period after a single dose with either vehicle (5% dextrose) or test compound at the specified doses. *$P < 0.05$, significantly different from vehicle control; one-way ANOVA with *post hoc* Dunnett's test; $n = 6–24$ animals per group.

When MCC was assessed at 1 h after dosing lactose (Figure 5A), the animals cleared the ^{99m}Tc-SC between 0 and 60 min after which time clearance appeared to halt. NVP-QBE170-treated animals showed a dose-dependent increase in the rate of clearance between 0 and 60 min after administration of ^{99m}Tc-SC with the maximal efficacy observed in the region of 1.5–3.0 mg. When ^{99m}Tc-SC clearance was assessed at 4 h after compound dosing (Figure 5B), the effect of NVP-QBE170 was apparent at doses ≥3 mg, with the greatest clearance observed at the highest dose studied, 12 mg. Blood K$^+$ levels were measured between 0 and 24 h after administration of NVP-QBE170 and were not significantly changed from the lactose control group (Supporting Information Fig. S3). The efficacy of inhaled hypertonic saline (7%) was also assessed in the MCC system (Figure 5C). When measured immediately after inhalation of 7% saline, MCC was significantly enhanced when compared with the water control. By 4 h after dosing, there was no residual effect of the hypertonic saline.

Pharmacokinetic profiles of NVP-QBE170 and P552-02

In rats, NVP-QBE170 showed a moderate volume of distribution (2.2 L·kg^{-1}) and was rapidly cleared with an elimination $t_{1/2}$ of 0.9 h (Table 6). P552-02 displayed a longer $t_{1/2}$ of 3.8 h and higher volume of distribution (19.7 L·kg^{-1}). Urinary elimination of the two compounds was also different with 0.97% and 33.3% of the administered doses of NVP-QBE170 and P552-02 being cleared by this route (as parent compound) respectively.
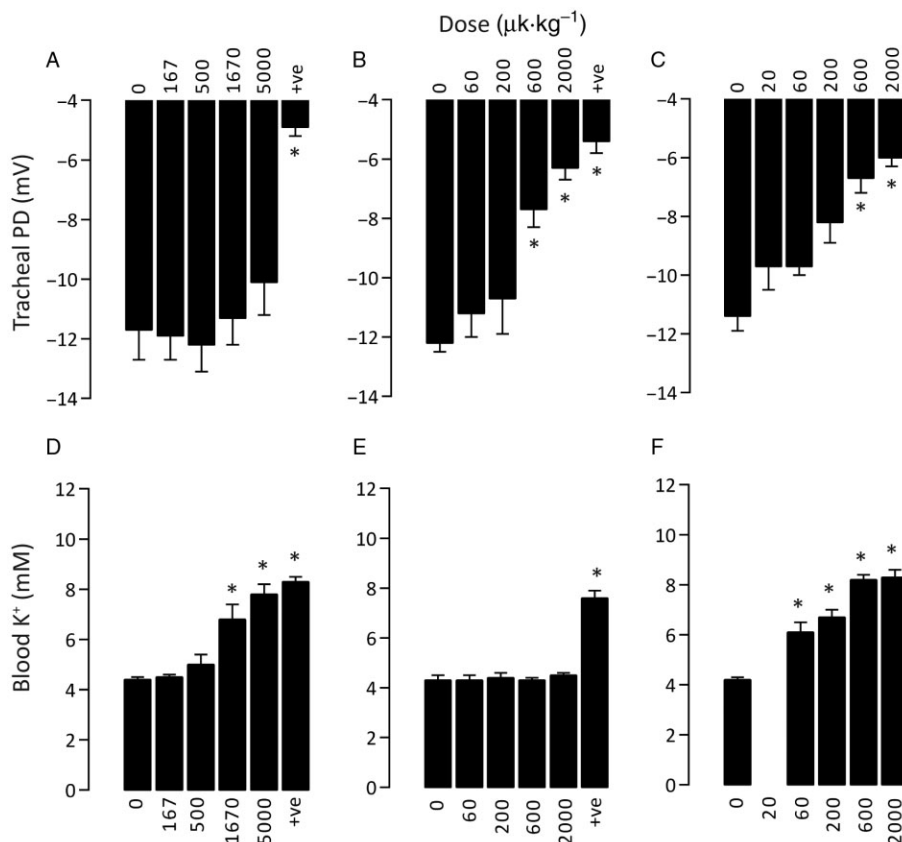
Figure 3

The *in vivo* effects of ENaC blockers on guinea pig TPD and blood potassium levels following i.t. dosing. TPD and blood potassium levels were measured in anaesthetized guinea pigs at 4 h after i.t. dosing with test compounds or vehicle. Absolute values for TPD and blood potassium are shown for amiloride (A and D), NVP-QBE170 (B and E), and P552-02 (C and F). +ve refers to the positive control compound in the study (P552-02, 2000 $\mu g \cdot kg^{-1}$). * $P < 0.05$, significantly different from vehicle (compound dose = 0 $\mu g \cdot kg^{-1}$); one-way ANOVA with *post hoc* Dunnett's test; $n = 4$–10 animals per group.

Discussion

The combination of functional studies from PHA type 1 patients (Kerem *et al.*, 1999) and compound data with inhaled amiloride (Köhler *et al.*, 1986; App *et al.*, 1990) and P552-02 (Donaldson *et al.*, 2005) suggests that block of ENaC in the airways increases MCC and thereby has the potential to enhance innate host defence. However, it is yet to be convincingly tested that airway ENaC block can provide clinical benefit in diseases characterized by impaired MCC, such as CF (Knowles *et al.*, 1990; Graham *et al.*, 1993; Bowler *et al.*, 1995). It has been proposed that amiloride failed to show robust clinical efficacy because of the combination of a short duration of action in the lung and the dose-limiting side effect of hyperkalaemia (Hirsh *et al.*, 2004). To enable the validity of the ENaC hypothesis to be tested therapeutically, ENaC blockers that are characterized by an improved duration of action in the lung and a reduced potential to induce hyperkalaemia will need to be developed. The recent termination of GS-9411 highlights the pressing need for such molecules (O'Riordan *et al.*, 2014).

NVP-QBE170 was designed as a potent ENaC blocker that could ultimately be delivered to the airways by inhalation as a dry powder. In addition to potency (>10-fold that of amiloride), key selection criteria were (i) evidence for an extended duration of action relative to amiloride, (ii) good species cross-reactivity to enable functional *in vivo* profiling; and (iii) a reduced potential to induce hyperkalaemia, again relative to amiloride. To achieve these criteria in the compound series, properties such as molecular weight (>600) and lipophilicity (LogD > 0.5) were used to guide compound design as they were considered to offer advantages in terms of reducing renal clearance and potentially enhancing lung residence time following inhalation.

NVP-QBE170 potently blocked the amiloride-sensitive I_{SC} in cultured human airway epithelial cells with an IC_{50} value of ~7 nM (>30-fold more potent than amiloride). Washout studies using primary HBEC cultures highlighted an extended duration of action of NVP-QBE170 relative to both P552-02 and amiloride. Of note, the duration of action of NVP-QBE170 was extended when the incubation time was increased (28.7% and 14.4% recovery following either a 2 or 10 min incubation respectively). Although a binding interaction between NVP-QBE170 and ENaC seems likely, in view of the potency shift in the presence of the αβG525Aγ or αβγG537C mutations (Schild *et al.*,
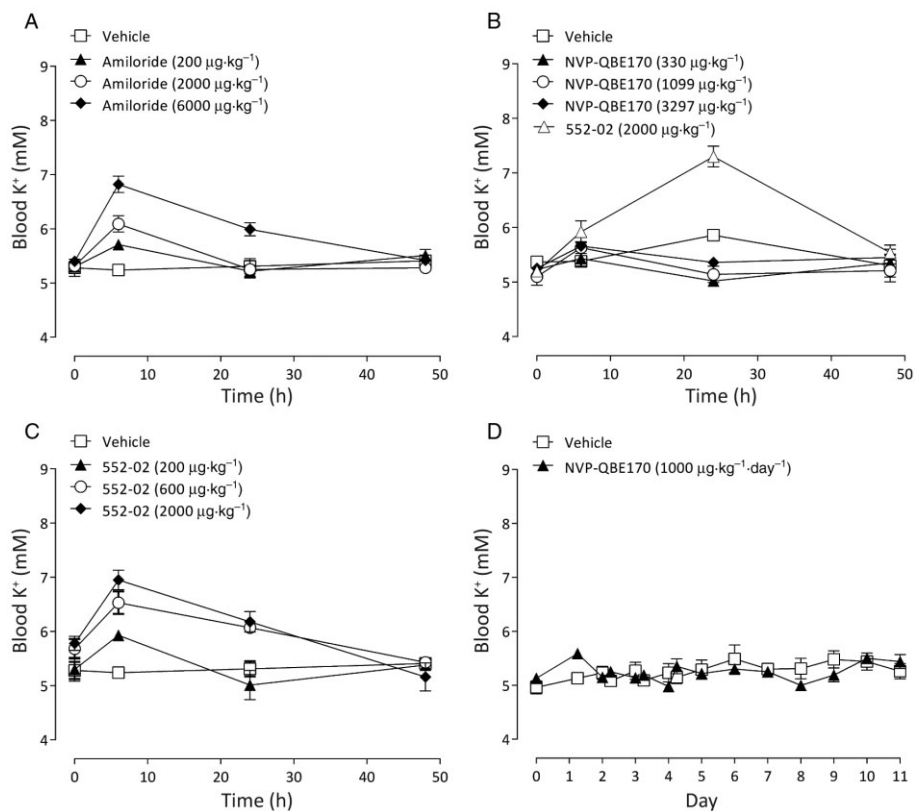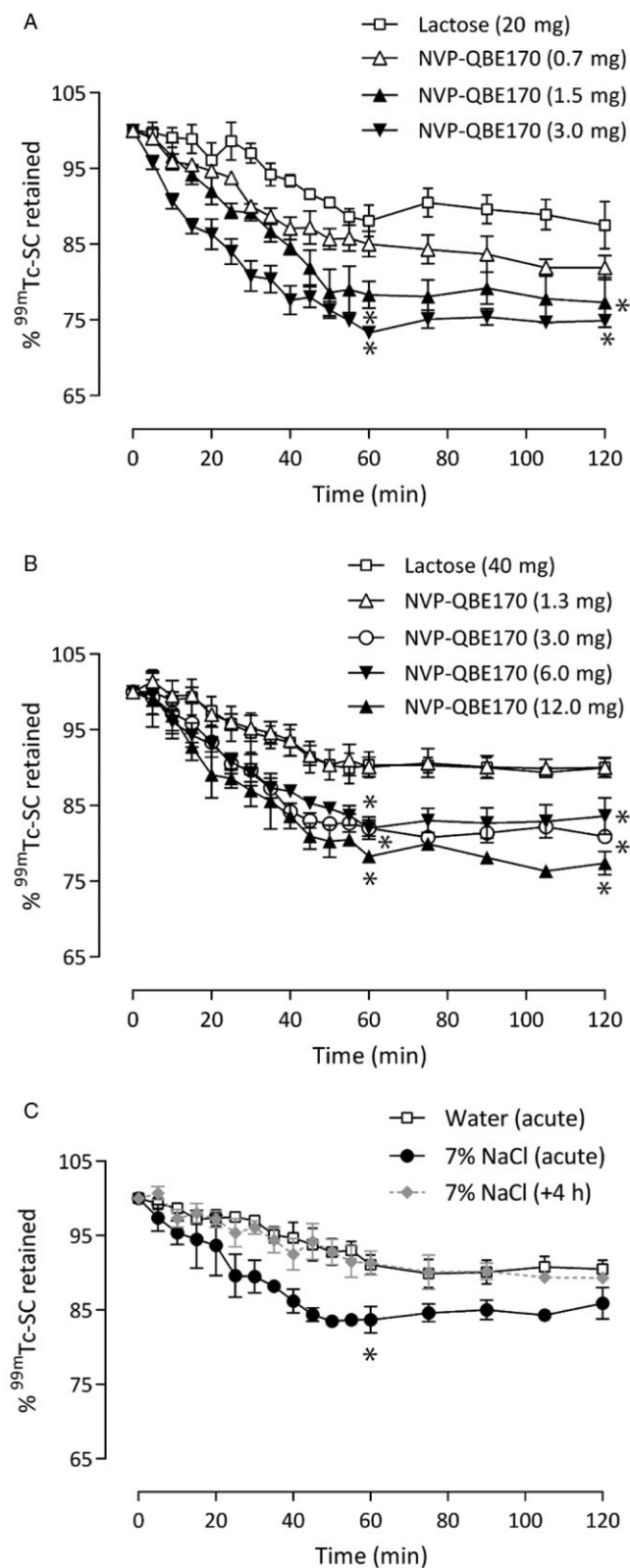
Figure 4
The effects of ENaC blockers on blood potassium levels in rats following i.t. dosing. Male Sprague-Dawley rats were dosed with test compounds or vehicle by i.t. administration. In addition to a pre-dose baseline level of blood potassium, samples were taken at 6, 24 and 48 h. The effects of a single dose of amiloride (A), NVP-QBE170 (B) and P552-02 (C) were studied as well as repeated daily dosing of NVP-QBE170 (D) for 10 days. Mean absolute data ± SEM for blood potassium levels are shown. Group sizes of four to six animals were used.

1997), whether the extended duration of action relates to altered kinetics on the channel or to membrane association of the compound and the maintenance of a high local concentration close to the target remains to be established. On this final point, Hirsh *et al.* (2008) reported a reduced off-rate from ENaC with P552-02 relative to amiloride using a patch clamp-based technique. This observation is consistent with the potential to design ENaC blockers with an extended duration of on-target engagement.

Further I_{SC} studies in HBEC confirmed that the forskolin and UTP-stimulated anion-secretory responses of the epithelium were similar irrespective of pretreatment with the ENaC blockers (Supporting Information Table S1). This is important considering that the related compound phenamil (Hirsh *et al.*, 2004) has been reported to attenuate the activity of the Na$^+$K$^+$-ATPase pump in the basolateral membrane, and thereby can suppress active ion transport processes. Amiloride analogues, such as 5-(N-ethyl-N-isopropyl) amiloride (EIPA) can also block the Na$^+$H$^+$ exchanger, NHE1 (Frelin *et al.*, 1988). None of the ENaC blockers tested showed any activity at NHE1 in two to three independent experiments, although autofluorescence of NVP-QBE170 prevented concentrations >3 μM being tested. EIPA did demonstrate activity in this assay as predicted (Supporting Information Table S2).

The excellent species cross-reactivity observed in the amiloride series of ENaC blockers enabled the use of *in vivo* models to begin to address salient questions relating to duration of action in the lung and hyperkalaemia following systemic exposure. We have previously reported that P552-02 (0.2 μg·kg^{-1}) and amiloride (16 μg·kg^{-1}) can acutely (1 h after dosing) block airway ENaC activity in the guinea pig using TPD as the readout (Coote *et al.*, 2008). Similarly, NVP-QBE170 also attenuated the TPD at 1 h after i.t. instillation with an ED$_{50}$ value of 1.7 μg·kg^{-1}. NVP-QBE170 is ~6-fold less potent than P552-02 on guinea pig ENaC *in vitro* (Table 1), consistent with their respective *in vivo* profiles. In a separate series of studies, TPD was measured at 4 h after dosing to examine the duration of compound effects. In these studies, both NVP-QBE170 and P552-02 still showed effects at 4 h (Figure 3B and C) that was in contrast to amiloride where there was no residual activity up to the highest dose that could be formulated (Figure 3A). It is likely that the extended duration of activity of NVP-QBE170 and P552-02 relative to amiloride *in vivo* is due to the combination of (i) greater on-target potency and therefore the ability to deliver a larger relative dose; and (ii) the greater duration of action relative to amiloride observed both in the present washout studies (Figure 2B and C) plus the reported patch clamp kinetic study for P552-02 (Hirsh *et al.*, 2008).

Figure 5

The effects of inhaled NVP-QBE170 and HS on MCC in conscious sheep. Mean retention of ^{99m}Tc labelled sulphur colloid ± SEM was measured by gamma scintigraphy in conscious sheep following administration of either inhaled NVP-QBE170 or HS. The assessment of clearance was started at either 1 h (A) or 4 h (B) after dosing with dry powder NVP-QBE170. The effect of inhaled 7% saline was assessed either immediately after inhalation of the osmolyte or at 4 h after dosing (C). Group sizes of three to five sheep per dose were used. *$P < 0.05$, significantly different from from vehicle control at either 60 or 120 min after ^{99m}Tc administration.

Inhibition of ENaC function in the renal cortical collecting duct leads to natriuresis and the accumulation of systemic potassium leading to hyperkalaemia, a potentially fatal condition (Perazella, 2000). As such, we also measured blood potassium levels in the 4 h animals to gain an early insight into the relative side effect liability of the test compounds. An early peak in potassium levels (~4 h after dosing) was reported in clinical studies with inhaled GS-9411 that would add relevance to the selection of this time point in a preclinical model (O'Riordan *et al.*, 2014). Considering that amiloride was originally designed as a potassium sparing diuretic, the observed elevation in potassium levels (Figure 3D) was not surprising, even after airway administration, as absorption into the systemic circulation and renal clearance are rapid (Hofmann *et al.*, 1997; Noone *et al.*, 1997). P552-02 also induced a dose-dependent elevation in potassium levels (Figure 3F) that would be consistent with exposure of the kidney to the parent compound and/or active metabolites. In contrast, NVP-QBE170 failed to induce a change in potassium levels at the time and doses tested (Figure 3E).

To test whether the relative lack of hyperkalaemia that was associated with NVP-QBE170 in the guinea pig was either species or time dependent, we established a model of hyperkalaemia in the rat. Similar to the observations in the guinea pig, amiloride and P552-02 induced hyperkalaemia in rats when given by i.t. instillation (Table 5). In contrast to both amiloride and P552-02, a single administration of NVP-QBE170 did not significantly elevate blood potassium levels up to the highest dose that could be formulated. To test the hypothesis that the reduced hyperkalaemia with NVP-QBE170 was due to reduced renal exposure, NVP-QBE170 and P552-02 were given i.v. to guarantee full systemic exposure to the administered dose and urinary elimination was assessed. These studies showed a greater degree of urinary elimination for P552-02 than for NVP-QBE170. The renal clearance of neutral and basic compounds is correlated with their physicochemical properties and degree of plasma protein binding (Varma *et al.*, 2009; Kusama *et al.*, 2010). A preference for renal clearance is associated with lower molecular weight (<600), lower LogD (<0.5) and lower plasma protein binding (<80%). The molecular weight and plasma protein binding of NVP-QBE170 (Supporting Information Table S3) fall outside of the preferred range for renal clearance while the lipophilicity (LogD) is borderline. Metabolite identification studies failed to detect significant levels of any NVP-QBE170 metabolites (data not shown). Biliary excretion of the parent molecule has been subsequently identified as the major route of elimination (data not shown). By contrast, the lower molecular weight and plasma protein binding of P552-02 (Supporting Information Table S3) are compatible with renal clearance, although the LogD is higher than typically observed with renally cleared drugs. Together, these data are

Table 6

Rat *in vivo* pharmacokinetic parameters for ENaC blockers

Compound	CL (mL·min⁻¹·kg⁻¹)	Vss (L·kg⁻¹)	$t_{1/2}$ (h)	Urinary clearance (% dose)
NVP-QBE170 (i.v.)	75.0 ± 37.7	2.2 ± 0.2	0.9 ± 0.48	$0.97 \pm (0–96\ h)$
P552-02 (i.v.)	149 ± 19	19.7 ± 4.9	3.8 ± 0.8	$33.7 \pm 7.3\ (0–24\ h)$

Mean ± SEM clearance (CL), volume of distribution at steady state (Vss), elimination $t_{1/2}$ and the urinary clearance of parent compound were calculated from independent studies using ^{14}C labelled NVP-QBE170 and unlabelled 552-02. $n = 3$ animals per compound.

consistent with a reduced urinary elimination (i.e. less renal exposure) of NVP-QBE170 driving the reduced potential to induce hyperkalaemia in rats.

Finally, we compared the efficacy and duration of action of dry powder NVP-QBE170 with hypertonic saline (7%) in a sheep model of MCC. The efficacy of novel mucokinetics relative to hypertonic saline is important as hypertonic saline has demonstrated clinical efficacy in several studies and is used by many patients with reported benefit. Specifically, hypertonic saline enhanced MCC and FEV_1 in a 4 week CF study (Donaldson *et al.*, 2006), and also reduced the exacerbation frequency in a 1 year study (Elkins *et al.*, 2006). In sheep, NVP-QBE170 induced a dose-dependent increase in MCC that could be sustained out to at least 4 h at higher doses (≥3 mg), without inducing hyperkalaemia. The efficacy was similar to that previously reported with P552-02 in this model (Hirsh *et al.*, 2008). Hypertonic saline induced an acute enhancement in MCC that was apparent when assessed immediately after the completion of dosing (i.e. no 1 h lag time between compound dosing and MCC assessment). The maximum efficacy of this dose of was however less than that of NVP-QBE170, and had totally disappeared by 4 h after the completion of dosing. Together, these data would be consistent with hypertonic saline providing a lower maximum effect and duration of action, relative to NVP-QBE170. A key question is whether the findings from the sheep model will translate into equivalent clinical efficacy, especially in view of the differences between the mechanism of action of an ENaC blocker and hypertonic saline, in addition to inherent differences between healthy sheep and the damaged airways of many CF patients. However, the efficacy of amiloride (in terms of enhanced MCC) did translate from healthy sheep to CF patients (Köhler *et al.*, 1986; App *et al.*, 1990; Hirsh *et al.*, 2004). In addition to providing the osmotic driving force to move water into the airway lumen, hypertonic saline is also an irritant and induces coughing in many patients which may be beneficial in helping to clear mucus out of the lungs. An inhaled ENaC blocker would not be expected to induce cough so it is likely to provide a different efficacy profile. Furthermore, hypertonic saline will act predominantly in the larger airways due to early deposition of the aerosol, as the droplets osmotically swell in the humidity of the airways. Inhaled ENaC blockers may therefore offer the potential to penetrate deeper into the airway tree providing effects across a broader spectrum of airway sizes that may provide additional benefit beyond that of hypertonic saline.

In summary, NVP-QBE170 exhibits many of the features that will be required in an inhaled ENaC blocker to appropri-

ately address the question of clinical efficacy with this therapeutic target. Long-term safety studies have halted the clinical development of NVP-QBE170, as 28-day inhalation safety studies revealed the potential for NVP-QBE170 to induce a local irritancy response in the airways. However, this molecule does highlight the potential of this design approach, enabling (i) potent and long-lasting block of ENaC relative to amiloride; (ii) greater efficacy and duration of action than with inhaled 7% saline *in vivo*; and (iii) the potential to diminish the risk of hyperkalaemia through the avoidance of renal clearance mechanisms.

Acknowledgements

Author contributions

K. C., D. P., S. C. and M. T.: Design, execution and interpretation of *in vivo* studies (guinea pig and rat). H. W., A. Y. and R. S.: Execution and interpretation of *in vitro* studies. P. G. K.: Generation of molecular reagents. M. G.: Design and interpretation of patch clamp studies. J. H. and A. S.: Design, execution and interpretation of NHE assay. C. P.: Biology strategy. B. E., R. L. and G. W.: Design, execution and interpretation of PK studies. W. A. and J. S.: Design, execution and interpretation of sheep MCC studies. N. S., M. V. and U. B.: Design and synthesis of NVP-QBE170. T. F.: Design of PK studies. S. C.: Medicinal chemistry strategy and interpretation of project data. H. D.: Biology strategy, design and interpretation of *in vitro/in vivo* studies/project data.

Conflict of interest

All authors, with the exception of W. A. and J. S., are current or historical employees of the Novartis Institutes of BioMedical Research. Novartis does not sell any of the test compounds or devices described in this manuscript.

References

Alexander SPH, Benson HE, Faccenda E, Pawson AJ, Sharman JL, Catterall WA *et al.* (2013a). The Concise Guide to PHARMACOLOGY 2013/14: Ion Channels. Br J Pharmacol 170: 1607–1651.

Alexander SPH, Benson HE, Faccenda E, Pawson AJ, Sharman JL Spedding M *et al.* (2013b). The Concise Guide to PHARMACOLOGY 2013/14: Enzymes. Br J Pharmacol 170: 1797–1867.

App EM, King M, Helfesrieder R, Köhler D, Matthys H (1990). Acute and long-term amiloride inhalation in cystic fibrosis lung disease. A rational approach to cystic fibrosis therapy. Am Rev Respir Dis 141: 605–612.

Boucher RC (2007). Evidence for airway surface dehydration as the initiating event in CF airway disease. J Intern Med 261: 5–16.

Boucher RC, Cotton CU, Gatzy JT, Knowles MR, Yankaskas JR (1988). Evidence for reduced Cl- and increased Na+ permeability in cystic fibrosis human primary cell cultures. J Physiol 405: 77–103.

Bowler IM, Kelman B, Worthington D, Littlewood JM, Watson A, Conway SP *et al.* (1995). Nebulised amiloride in respiratory exacerbations of cystic fibrosis: a randomised controlled trial. Arch Dis Child 73: 427–430.

Canessa CM, Horisberger JD, Rossier BC (1993). Epithelial sodium channel related to proteins involved in neurodegeneration. Nature 361: 467–470.

Chang SS, Grunder S, Hanukoglu A, Rösler A, Mathew PM, Hanukoglu I *et al.* (1996). Mutations in subunits of the epithelial sodium channel cause salt wasting with hyperkalaemic acidosis, pseudohypoaldosteronism type 1. Nat Genet 12: 248–253.

Chen JH, Stoltz DA, Karp PH, Ernst SE, Pezzulo AA, Moninger TO *et al.* (2010). Loss of anion transport without increased sodium absorption characterizes newborn porcine cystic fibrosis airway epithelia. Cell 143: 911–923.

Coote K, Atherton-Watson HC, Sugar R, Young A, MacKenzie-Beevor A, Gosling M *et al.* (2009). Camostat attenuates airway epithelial sodium channel function *in vivo* through the inhibition of a channel-activating protease. J Pharmacol Exp Ther 329: 764–774.

Coote KJ, Atherton H, Young A, Sugar R, Burrows R, Smith NJ *et al.* (2008). The guinea-pig tracheal potential difference as an *in vivo* model for the study of epithelial sodium channel function in the airways. Br J Pharmacol 155: 1025–1033.

Donaldson S, Smith R, Doran J, DiMassimo B, Zeman K, Bennett B *et al.* (2005). Safety, pharmacokinetics and effects on mucus clearance following administration of 552-02 to normal healthy volunteers. Pediatr Pulmonol 40: 218, Abstract.

Donaldson SH, Bennett WD, Zeman KL, Knowles MR, Tarran R, Boucher RC (2006). Mucus clearance and lung function in cystic fibrosis with hypertonic saline. N Engl J Med 354 (3): 241–250.

Elkins MR, Robinson M, Rose BR, Harbour C, Moriarty CP, Marks GB *et al.* (2006). A controlled trial of long-term inhaled hypertonic saline in patients with cystic fibrosis. N Engl J Med 354: 229–240.

Frelin C, Barbry P, Vigne P, Chassande O, Cragoe EJ Jr, Lazdunski M (1988). Amiloride and its analogs as tools to inhibit Na+ transport via the Na+ channel, the Na+/H + antiport and the Na+/Ca2+ exchanger. Biochimie 70: 1285–1290.

Graham A, Hasani A, Alton EW, Martin GP, Marriott C, Hodson ME *et al.* (1993). No added benefit from nebulized amiloride in patients with cystic fibrosis. Eur Respir J 6: 1243–1248.

Hirsh A (2002). Altering airway surface liquid volume: inhalation therapy with amiloride and hyperosmotic agents. Adv Drug Deliv Rev 54: 1445–1462.

Hirsh AJ, Sabater JR, Zamurs A, Smith RT, Paradiso AM, Hopkins S *et al.* (2004). Evaluation of second generation amiloride analogs as therapy for cystic fibrosis lung disease. J Pharmacol Exp Ther 311: 929–938.

Hirsh AJ, Zhang J, Zamurs A, Fleegle J, Thelin WR, Caldwell RA *et al.* (2008). Pharmacological properties of N-(3,5-diamino-6-chloropyrazine-2-carbonyl)-N'-4-[4-(2,3-dihydroxypropoxy)phenyl] butyl-guanidine methanesulfonate (552-02), a novel epithelial sodium channel blocker with potential clinical efficacy for cystic fibrosis lung disease. J Pharmacol Exp Ther 325: 77–88.

Hofmann T, Senier I, Bittner P, Hüls G, Schwandt HJ, Lindemann H (1997). Aerosolized amiloride: dose effect on nasal bioelectric properties, pharmacokinetics, and effect on sputum expectoration in patients with cystic fibrosis. J Aerosol Med 10: 147–158.

Itani OA, Chen JH, Karp PH, Ernst S, Keshavjee S, Parekh K *et al.* (2011). Human cystic fibrosis airway epithelia have reduced Cl-conductance but not increased Na+ conductance. Proc Natl Acad Sci U S A 108: 10260–10265.

Jespersen T, Grunnet M, Angelo K, Klaerke DA, Olesen SP (2002). Dual-function vector for protein expression in both mammalian cells and *Xenopus laevis* oocytes. Biotechniques 32: 536–538, 540.

Kellenberger S, Schild L (2002). Epithelial sodium channel/degenerin family of ion channels: a variety of functions for a shared structure. Physiol Rev 82: 735–767.

Kerem E, Bistritzer T, Hanukoglu A, Hofmann T, Zhou Z, Bennett W *et al.* (1999). Pulmonary epithelial sodium-channel dysfunction and excess airway liquid in pseudohypoaldosteronism. N Engl J Med 341: 156–162.

Kilkenny C, Browne W, Cuthill IC, Emerson M, Altman DG (2010). Animal research: reporting *in vivo* experiments: the ARRIVE guidelines. Br J Pharmacol 160: 1577–1579.

Knowles M, Gatzy J, Boucher R (1981). Increased bioelectric potential difference across respiratory epithelia in cystic fibrosis. N Engl J Med 305: 1489–1495.

Knowles MR, Church NL, Waltner WE, Yankaskas JR, Gilligan P, King M *et al.* (1990). A pilot study of aerosolized amiloride for the treatment of lung disease in cystic fibrosis. N Engl J Med 322: 1189–1194.

Köhler D, App E, Schmitz-Schumann M, Würtemberger G, Matthys H (1986). Inhalation of amiloride improves the mucociliary and the cough clearance in patients with cystic fibroses. Eur J Respir Dis Suppl 146: 319–326.

Kusama M, Toshimoto K, Maeda K, Hirai T, Imai S, Chiba K *et al.* (2010). In Silico Classification of major clearance pathways of drugs with their physiochemical parameters. Drug Metab Dispos 38: 1362–1370.

Mall M, Grubb BR, Harkema JR, O'Neal WK, Boucher RC (2004). Increased airway epithelial Na+ absorption produces cystic fibrosis-like lung disease in mice. Nat Med 10: 487–493.

Matsui H, Grubb BR, Tarran R, Randell SH, Gatzy JT, Davis CW *et al.* (1998). Evidence for periciliary liquid layer depletion, not abnormal ion composition, in the pathogenesis of cystic fibrosis airways disease. Cell 95: 1005–1015.

McGrath JC, Drummond GB, McLachlan EM, Kilkenny C, Wainwright CL (2010). Guidelines for reporting experiments involving animals: the ARRIVE guidelines. Br J Pharmacol 160: 1573–1576.

Noone PG, Regnis JA, Liu X, Brouwer KL, Robinson M, Edwards L *et al.* (1997). Airway deposition and clearance and systemic pharmacokinetics of amiloride following aerosolization with an ultrasonic nebulizer to normal airways. Chest 112: 1283–1290.

O'Riordan TG, Donn KH, Hodsman P, Ansede JH, Newcomb T, Lewis SA *et al.* (2014). Acute hyperkalemia associated with inhalation of a potent ENaC antagonist: phase 1 trial of GS-9411. J Aerosol Med Pulm Drug Deliv 27: 200–208.

Pawson AJ, Sharman JL, Benson HE, Faccenda E, Alexander SP, Buneman OP *et al.*; NC-IUPHAR (2014). The IUPHAR/BPS Guide to PHARMACOLOGY: an expert-driven knowledge base of drug targets and their ligands. Nucl Acids Res 42 (Database Issue): D1098–D1106.

Perazella MA (2000). Drug-induced hyperkalemia: old culprits and new offenders. Am J Med 109: 307–314.

Pons G, Marchand MC, d'Athis P, Sauvage E, Foucard C, Chaumet-Riffaur P *et al.* (2000). Amiloride-AFLM Collaborative Study Group: French multicenter randomized double-blind placebo-controlled trial on nebulized amiloride in cystic fibrosis patients. Pediatr Pulmonol 30: 25–31.

Quinton PM (1989). Defective epithelial ion transport in cystic fibrosis. Clin Chem 35: 726–730.

Riordan JR, Rommens JM, Kerem B, Alon N, Rozmahel R, Grzelczak Z *et al.* (1989). Identification of the cystic fibrosis gene: cloning and characterization of complementary DNA. Science 245: 1066–1073.

Schild L, Schneeberger E, Gautschi I, Firsov D (1997). Identification of amino acid residues in the alpha, beta, and gamma subunits of the epithelial sodium channel (ENaC) involved in amiloride block and ion permeation. J Gen Physiol 109: 15–26.

Sheppard DN, Carson MR, Ostedgaard LS, Denning GM, Welsh MJ (1994). Expression of cystic fibrosis transmembrane conductance regulator in a model epithelium. Am J Physiol 266: L405–L413.

Staruschenko A, Booth RE, Pochynyuk O, Stockand JD, Tong Q (2006). Functional reconstitution of the human epithelial Na+ channel in a mammalian expression system. Methods Mol Biol 337: 3–13.

Strautnieks SS, Thompson RJ, Gardiner RM, Chung E (1996). A novel splice-site mutation in the gamma subunit of the epithelial sodium channel gene in three pseudohypoaldosteronism type 1 families. Nat Genet 13: 248–250.

Varma MVS, Feng BR, Obach RS, Troutman MD, Chupka J, Miller HR *et al.* (2009). Physicochemical determinants of human renal clearance. J Med Chem 52: 4844–4852.

Zhou Z, Treis D, Schubert SC, Harm M, Schatterny J, Hirtz S *et al.* (2008). Preventive but not late amiloride therapy reduces morbidity and mortality of lung disease in betaENaC-overexpressing mice. Am J Respir Crit Care Med 178: 1245–1256.

Supporting information

Additional Supporting Information may be found in the online version of this article at the publisher's web-site:

http://dx.doi.org/10.1111/bph.13075

Figure S1 Sample raw data trace illustrating the effects of NVP-QBE170 on the ENaC-mediated short-circuit current in human airway epithelial cells.

Figure S2 Sample raw data traces illustrating the different washout profiles of amiloride, P552-02 and NVP-QBE170 following incubation with primary HBE.

Figure S3 The effects of lactose and NVP-QBE170 on blood K^+ levels in sheep following inhaled dosing as a dry powder.

Table S1 The effects of NVP-QBE170 on anion-secretory responses in human bronchial epithelial cells.

Table S2 The effects of NVP-QBE170 on Na^+/H^+ exchanger activity.

Table S3 Molecular properties and *in vitro* pharmacokinetic parameters for ENaC blockers.